Environmental Science
Water Research & Technology

ROYAL SOCIETY OF CHEMISTRY

PAPER

View Article Online
View Journal | View Issue

Check for updates

Cite this: *Environ. Sci.: Water Res. Technol.*, 2022, **8**, 1300

Effect of sodium silicate on drinking water biofilm development†

Sebastian Munoz, Benjamin F. Trueman, Bofu Li and Graham A. Gagnon *

Sodium silicates have been studied as drinking water additives for coagulation, sequestration of iron, and corrosion control, but their impact on biofilm formation has received less attention. This study investigated the impact of sodium silicate corrosion control on biomass accumulation in comparison to orthophosphate, a common corrosion inhibitor. Biofilm growth was measured by determining ATP concentrations, and bacterial communities were characterized using 16S ribosomal RNA (rRNA) sequencing. In a pilot-scale study with annular reactors (ARs) fed by cast iron pipe loops, biofilm ATP concentrations were substantially lower on polycarbonate coupons in the sodium silicate-treated AR than on those in the orthophosphate-treated AR when the water temperature exceeded 20 °C. An elevated sodium silicate dose (48 mg L^{-1} of SiO_2), however, dispersed the biofilm, resulting in elevated effluent ATP concentrations. Two separate experiments confirmed that biomass accumulation was higher in the presence of orthophosphate at high water temperatures (≥20 °C), whereas no significant differences were identified in biofilm ATP concentrations at lower water temperatures (<20 °C). Differences in bacterial communities between the orthophosphate- and sodium silicate-treated systems were not statistically significant, even though orthophosphate promoted higher biofilm growth. The genera *Halomonas* and *Mycobacterium*, however—which include opportunistic pathogens—were present at greater relative abundances in the orthophosphate- compared to the silicate-treated system.

Received 20th September 2021,
Accepted 3rd May 2022

DOI: 10.1039/d1ew00682g

rsc.li/es-water

Water impact

Sodium silicates have been used in drinking water treatment for decades, both as sequestrants and as corrosion inhibitors. A poor understanding of their impact on biofilm formation, however, constitutes a risk to drinking water quality. This study helps to clarify the effects of silicate- and phosphate-based corrosion inhibitors on biofilm development.

Introduction

Internal corrosion of distribution pipes can release lead, copper, and iron into drinking water. It can also result in tubercles—deposited corrosion products—which accumulate biofilms and provide an environment for bacteria and opportunistic pathogens.[1,2] Corrosion by-products can react with disinfectant, neutralizing it before it can inactivate microorganisms in the bulk water or biofilm.[1,3,4] To mitigate corrosion, drinking water treatment plants may adjust pH and alkalinity or dose a corrosion inhibitor (or in some cases, both). According to a 2019 corrosion control survey, 54% of US utilities use a phosphate-based corrosion inhibitor.[5]

Centre for Water Resources Studies, Department of Civil & Resource Engineering, Dalhousie University, 1360 Barrington St., Halifax, Nova Scotia, Canada B3H 4R2. E-mail: graham.gagnon@dal.ca

† Electronic supplementary information (ESI) available: Figures summarizing water quality data, taxonomic analysis, and diversity analysis. See DOI: https://doi.org/10.1039/d1ew00682g

While in most cases organic carbon limits biofilm growth in drinking water distribution systems, phosphorus has also been identified as the growth-limiting nutrient.[6–9] Studies have shown that phosphate promotes bacterial diversity as well as biofilm growth,[7,10] but others are contradictory.[11] Some work suggests that phosphate neither influences total bacterial densities,[2,12] nor supports biofilm growth.[13] These inconsistencies motivate further investigation of the effects of corrosion inhibitors on biofilm development, including inhibitors that are not phosphate-based.

Sodium silicates are used primarily for iron/manganese sequestration and coagulation, but they have been used occasionally as alternatives to orthophosphate;[14] in particular, they have been evaluated for lead release control with mixed results.[15–19] Sodium silicates may inhibit the oxidation of ferrous iron, particularly in the pH range of 6.0–7.0,[20] and they may also reduce color and water turbidity.[21]

While some focus has been directed to understanding sodium silicates as corrosion inhibitors, their impact on

biofilm formation has received comparatively little attention. Several studies do suggest that silicate treatment exerts a minimal influence on biofilm: Rompré *et al.*[2] reported that sodium silicate did not influence biofilm growth in comparison to orthophosphate and blended *ortho*-polyphosphate inhibitors, suggesting that biofilm accumulation is influenced more by the substrate material than the corrosion inhibitor. Similarly, Kogo *et al.*[22] reported no significant difference in adenosine triphosphate (ATP) concentrations from biofilm samples among the orthophosphate, zinc orthophosphate, and sodium silicate-treated systems.

The main objective of this work was to compare the impact of sodium silicate on biomass accumulation in drinking water systems against orthophosphate, as measured by ATP concentrations and 16S ribosomal RNA (rRNA) sequencing analysis for bacterial community characterization. A pilot-scale study is presented in this paper to describe the impacts of sodium silicates on biofilm growth using water from a drinking water treatment plant. Our specific objectives were:

1. To study biofilm growth in the presence of sodium silicate, using a pilot-scale model distribution system comprising cast-iron pipe loops feeding rotating annular reactors (ARs). Biomass accumulation inside the ARs was monitored over a 10 month period that included seasonal water temperature variation.

2. To monitor, in the same model system, the biomass accumulated at low water temperatures (below 20 °C) on polycarbonate coupons representing PVC and cast-iron pipe loops treated with sodium silicate or orthophosphate.

A bench-scale experiment with the same filtered water used in the pipe loop system was completed using batch reactors and polyethylene (PEX) coupons. The objectives of this experiment were:

1. To complement the findings from the pilot study by measuring the biomass accumulated on PEX coupons treated with sodium silicate or orthophosphate.

2. To replicate the biomass accumulation on coupons exposed to high water temperatures (20 °C).

Materials and methods

Model distribution system

Pipe loop system. Water from the clearwell of the J. D. Kline Water Supply Plant (JDKWSP) (Halifax, Nova Scotia, Canada) was used to feed the pilot distribution system. JDKWSP uses alum coagulation followed by dual media direct filtration (sand and anthracite); the feedwater was diverted to the model system after these treatment steps but before final chemical (*e.g.*, orthophosphate, free chlorine) addition. A detailed description of the facility can be found in Knowles *et al.*,[23] and Stoddart *et al.*[24] The model distribution system comprised four independent pipe loops: two unlined cast-iron and two PVC pipe distribution main sections arranged in parallel (Fig. 1) and designed to simulate water aging in a drinking water distribution system. The iron distribution main sections were 150 mm in diameter and moderately to heavily tuberculated, whereas the PVC sections were 100 mm in diameter. Both types of distribution mains were approximately 1.8 m in length. The hydraulic retention time (HRT) in the loops was set at 12 hours, with water flowing in through the main pipes at a rate of 0.03 m s^{-1} (approximate values). A detailed description of the pipe

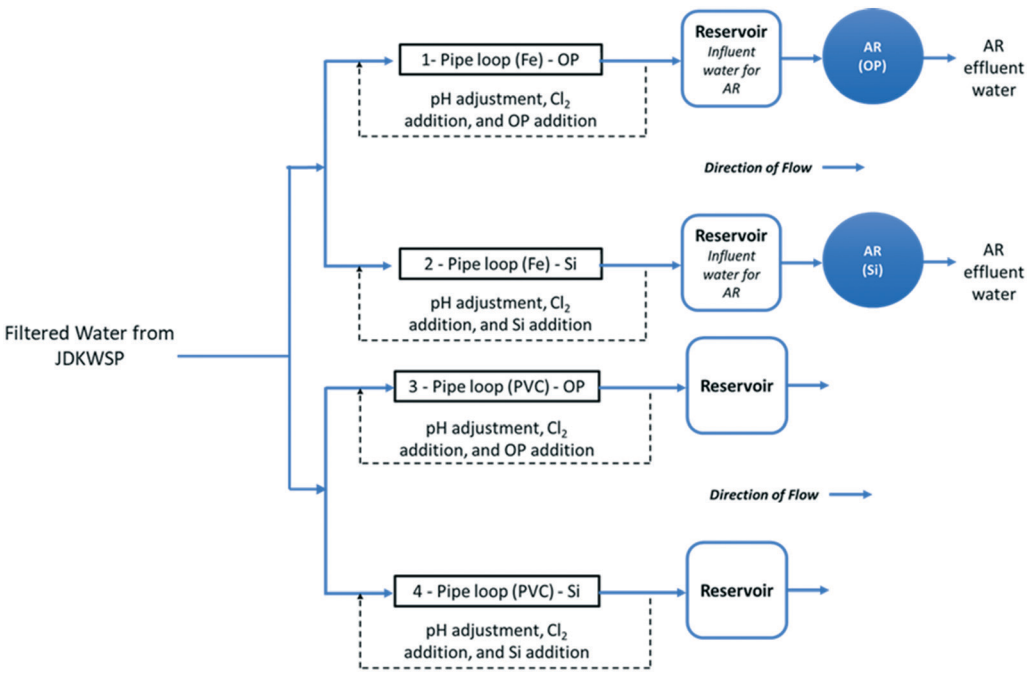

Fig. 1 Simplified schematic of the pipe loop system.

loop apparatus can be found in Gagnon *et al.*,[25] Woszczynski *et al.*,[26] and Trueman *et al.*[27]

Filtered water from JDKWSP was dosed twice per week with sodium hypochlorite and sodium hydroxide and with either phosphoric acid (pipe loops 1 and 3, Fig. 1) or sodium silicate (pipe loops 2 and 4) before entering the pipe loops. Residual concentrations of 1.0 mg L^{-1} free chlorine, a pH of 7.4, 1.0 mg L^{-1} PO_4^{3-}, and 24 mg L^{-1} SiO_2 were targeted in pipe loop effluent. These values fall within the typical range for drinking water.[28,29] In the final stage of the experiment, the SiO_2 residual target was increased to 48 mg L^{-1} to investigate the effect of sodium silicates on biofilm formation at higher doses. Further information about the model distribution system and a graphical water quality summary of this system can be found in Li *et al.*[15]

Two ARs—one for each corrosion inhibitor treatment (Fig. 1)—were fed from reservoirs at the effluent end of the cast-iron pipe loops. These ARs were used to assess the effect of each corrosion inhibitor on biofilm formation in a cast-iron main distribution system. Polycarbonate coupons were suspended in the reservoirs from all four pipe loops to identify the impact of pipe material on biofilm development.

Annular reactors. ARs have been successfully used as bench-scale models to mimic water distribution systems and to simulate biofilm growth in a variety of aquatic environments including drinking water systems, hulls of ships, and river ecosystems.[30–33] The ARs used in this study were manufactured by BioSurface Technologies Corporation (Model 1320 LS, Bozeman, MT, USA). The ARs comprised an inner, slotted polycarbonate cylinder with a stationary glass outer cylinder. Twenty removable polycarbonate slides were used to support biofilm growth. These coupons were extracted and analyzed to determine biofilm ATP concentrations and microbial community structures.

The ARs were connected in December 2018 and acclimated for 3 months before the bulk water and the first set of coupons were sampled in March 2019. This acclimation period was selected to ensure biofilm growth in the presence of residual free chlorine for disinfection. A total operating volume of approximately 950 mL was used for all AR experiments. With this working volume, the HRT of the reactors was set to two hours by pumping water at a flow rate of 7.9 mL min^{-1}. This HRT has been commonly used in various experiments to test biofilm growth under different water treatment and operational conditions.[30,33–35] The rotational speed of the reactors was set to 50 RPM, and influent/effluent water quality is summarized in Fig. S1 and S2.†

Before use, the ARs, fittings, tubing, flow breaks, and coupons were thoroughly cleaned with phosphorus-free detergent and rinsed with deionized water. All non-metal components of the ARs were then immersed in a 10% nitric acid solution for 24 hours and rinsed with deionized water. The assembled ARs and mounted coupons were fitted with Masterflex PerfectPosition Norprene tubing (Cole-Parmer Canada Company, QC, Canada) and autoclaved at 121 °C for 15 minutes. Once autoclaved and cooled, all non-opaque surfaces were covered with aluminum foil to reduce phototrophic growth within the reactors.[33] Peristaltic pumps (Cole-Parmer Canada Company, QC, Canada) were calibrated to feed the appropriate flow rates, and the reactors were fine-tuned to achieve the appropriate rotational speed.

One coupon from each AR was sampled every second week from March 2019 until the end of June 2019, after a three-month acclimation period that started in December 2018. The sampling frequency increased to one coupon per week after July 2019. During this period the coupons were extracted to quantify and compare total ATP (tATP) by sampling approximately 4.2 cm^2 of each of the coupon's exposed surface area.

The coupons were aseptically removed from the ARs with a flame-sterilized metal hook and placed in 150 mL sterile test tubes. Each test tube was filled with effluent water to prevent biofilm from drying. The test tubes carrying the coupons were transported in an ice-packed cooler to Dalhousie University for analysis. All microbiological tests were performed within 24 hours of sample collection inside a biological safety cabinet (BSC) to limit biological contamination of samples and maintain sterility of materials. Once biofilm collection from the coupons was completed, the coupons were cleaned with phosphorus-free detergent, rinsed with deionized water (reference A+, Milli-Q, Millipore), and disinfected with 70% ethanol. The coupons were then autoclaved at 121 °C for 15 minutes. Once cooled, the coupons were re-inserted into the ARs.

Reservoir-suspended coupons. To evaluate biomass accumulation under low water temperature conditions and different pipe materials, 14 removable polycarbonate coupons were suspended from the top of each reservoir (Fig. 1). All polycarbonate coupons were autoclaved at 121 °C for 15 minutes before use. The coupons were suspended and submerged in October 2019 inside the reservoirs using nylon fishing lines and wooden clamps. The majority of the surface area of these coupons (approximately 25 cm^2) was used to assess the biomass accumulated from each treated pipe loop system.

For this specific assessment, two polycarbonate coupons per reservoir were assessed weekly from October to November 2019 to compare the impact of pipe loop material (cast-iron *vs.* PVC) on biomass accumulation using tATP quantification. Coupons completed a 15 day conditioning period before the first set of samples was collected and analyzed. The collection process used for the coupons from the ARs was again applied for this part of the study.

Batch reactors

Biofilm growth at bench-scale was evaluated using amber glass reactors with annular PEX coupons by measuring the accumulated biomass as tATP. All components of the reactors were immersed in a 10% nitric acid solution for 24 hours and rinsed with deionized water. The assembled batch

reactors and coupons were autoclaved at 121 °C for 15 minutes. The reactors were stored in the dark and amber glass was used to limit the effects of light on phototrophic bacteria growth. Four coupons were inserted per reactor and each coupon had an internal surface area of approximately 28–30 cm^2, which was used for biofilm sampling (Fig. S3†). The test solutions (300 mL per reactor) comprised filtered water from the JD Kline water supply plant modified with orthophosphate (2 mg P per L) and sodium silicate (25 mg SiO_2 per L) at 20 °C. As a final step, pH was adjusted to 8 with 0.1 M NaOH. Free chlorine was dosed at 1 mg L^{-1} free chlorine and allowed to deplete over the experiment. The solution in the reactors was replaced daily using a dump and fill procedure. The coupons were acclimated for one month, under the experimental conditions, before collecting the samples.

Adenosine triphosphate analysis

Total ATP (tATP) was used as an indicator of total sessile biomass concentration accumulated on the surface of the coupons. Gora *et al.*[36] reported that swabbing was superior to scraping for biofilm recovery; thus, the exposed surface area of the coupons was swabbed for biofilm recovery and total ATP analysis. The extracted biofilm samples were then processed using LuminUltra Technologies' Deposit & Surface Analysis (DSA) test kit and protocol (New Brunswick, Canada), and analysed with their PhotonMaster luminometer to obtain data in relative light units (RLU). RLU were then translated to tATP concentrations (pg ATP per cm^2) using LuminUltra's conversion formula. The detection limit for this method is 10 RLU.

Bioinformatic analysis

At the beginning of each month from June – December 2019, 16S rRNA sequencing and bacterial species identification were performed on biofilm extracted from the surface of the AR coupons. Seven coupons—one per month—were extracted from each AR. These coupons were sampled on the first week of each month to identify any variations in the microbial community structure at the highest average tATP concentrations (July to September). For this analysis, the full surface area of the coupons was swabbed to extract the largest amount of biomass. DNA extraction was performed using the procedure outlined by the commercially available DNeasy PowerBiofilm Kit (QIAGEN, Hilden, Germany). All extracted DNA samples were sent to the Integrated Microbiome Resource (IMR) Laboratory at Dalhousie University for marker gene sequencing, using PCR V4–V5 primers that target the 16S ribosomal RNA (rRNA) gene in bacteria.

Results from the microbial community sequence were processed using the Microbiome Helper workflow[37] specific to 16S analysis.[37] First, cutadapt[38] was used to remove primer sequences from sequencing reads. The trimmed primer files were imported into QIIME2 for microbiome analysis.[39] Then, forward and reverse paired-end reads were joined using DADA2,[40] and input into Deblur[41] to correct reads and obtain amplicon sequence variants (ASVs). ASVs with frequencies lower than 0.1% of the mean sample depth were excluded from further analysis. MAFFT[42] was used to build a multiple-sequence alignment of ASVs and taxonomy was assigned to ASVs using the SILVA rRNA gene database[43] and the "feature-classifier" option in QIIME2. Further data processing and visualization were completed with the Phyloseq package in R.[44] Alpha diversity metrics including richness, Shannon's diversity index, and Pielou's evenness index were also analyzed. The Shannon diversity index describes species diversity within a community while taking richness (number of species present) into account. The Pielou index ranges from 0 to 1 and indicates how even the distribution of species is within a community. When the Pileou index approaches 0, it means that the community is dominated by a small subset of the total number of species (less evenness).

Water quality parameters

Aqueous samples were collected in 500 mL high-density polyethylene (HDPE) bottles once per week. Before use, sampling bottles were immersed in a 10% nitric acid solution for 24 hours and rinsed three times with deionized water. Samples collected from the JDKWSP were stored in an ice-packed cooler and transported to Dalhousie University (Halifax, Nova Scotia, Canada) for further analysis.

pH and temperature were measured immediately after sampling. pH was measured using an Accumet XL-50 dual-channel meter (Fisher Scientific, MA, USA) according to the manufacturer's instructions with a calibration completed each day before use. Temperature was measured using an alcohol thermometer.

Free chlorine, phosphate, and silica were also measured immediately after sampling using a DR6000 spectrophotometer (HACH, CO, USA), following the DPD method (Hach Method 8021), PhosVer 3 method (Hach Method 8048), and Silicomolybdate method (Hach Method 8185), respectively. The analytical ranges for these methods are 0.02–2.00 mg L^{-1} for Cl_2, 0.02–2.50 mg L^{-1} for orthophosphate, and 1–100 mg L^{-1} for SiO_2.[45–47]

To measure ATP concentrations in bulk water, aliquots of water (at least 50 mL) were collected in sterile falcon tubes. Cellular ATP (cATP) was used as an indicator of planktonic cell concentrations in aqueous samples. cATP was measured using LuminUltra Technologies' (New Brunswick, Canada) Quench-Gone Aqueous (QGA) test kit and protocol, along with their PhotonMaster luminometer. RLU were translated to ATP concentrations (pg ATP per mL) using LuminUltra's conversion formula. The detection limit for this method is 10 RLU.

Standards and reagents

Stock solutions of sodium hydroxide (1 M) (Fisher Scientific, MA, USA), sodium hypochlorite (Atlantic Chemical and

Aquatics Inc., NB, Canada), phosphoric acid (0.05 M) (Fisher Scientific, MA, USA), and sodium silicate solution (Na_2O : SiO_2 = 1 : 3.22, weight ratio) (National Silicates, ON, Canada), were made each week and diluted with feedwater to achieve the desired residual water quality concentrations.

Data analysis

Experimental data were analyzed using R (Version 3.6.2) (R Core Team, Vienna, Austria) and a variety of widely-used contributed packages.[44,48–50] Wilcoxon-signed rank tests (wilcox.test() in R) were used to compare paired samples under the assumption that repeated measurements from individual annular reactors were independent. Violation of this assumption tends to inflate the type I error rate (incorrect rejection of the null hypothesis). Since no statistical test on AR time series data resulted in a rejection of the null hypothesis, we did not evaluate the validity of the independence assumption in detail.[51] Correlations were calculated using Pearson's product – moment correlation coefficient (cor() in R). All statistical analyses were conducted at the 95% confidence level (α = 0.05).

Differences in alpha diversity (species richness, diversity, and evenness) between groups were calculated using Wilcoxon-signed rank tests with correction for false discovery rate (FDR). Beta diversity (community composition) was assessed using weighted and unweighted UniFrac principal coordinate analysis (PCoA) to explore similarities among samples. Unweighted UniFrac is based on the presence/absence of different taxa and abundance is not considered, while the weighted UniFrac considers the abundance of different taxa.[52,53] Differences in beta diversity were calculated applying a permutational ANOVA (PERMANOVA) Adonis test, which is a non-parametric multivariate analysis of variance that compares the abundance of each taxon in a sample to its abundance in other samples.[54]

Results and discussion

Impact of sodium silicate on biofilm formation in a pilot-scale system (annular reactors)

Cellular ATP (cATP) and biofilm ATP (tATP). While cellular ATP concentrations were similar in reactors treated with sodium silicate and orthophosphate, biofilm ATP concentrations were greater in the presence of orthophosphate (Fig. 2a and b). Cellular ATP concentrations increased in the effluent of both ARs during the July–September quarter. The median cellular ATP concentrations were 2.12 pg cATP per mL (range: 0.06–36.3 pg cATP per mL, n = 66) and 1.84 pg cATP per mL (range: 0.07–68.0 pg cATP per mL, n = 66) in effluent from the orthophosphate- and sodium silicate-treated ARs, respectively. A Wilcoxon-signed rank test confirmed that this difference was not statistically significant ($p > 0.05$). However, an immediate spike in effluent cellular ATP from the sodium silicate-treated AR was evident after the sodium silicate dose was doubled at the beginning of September (Fig. 2b). This

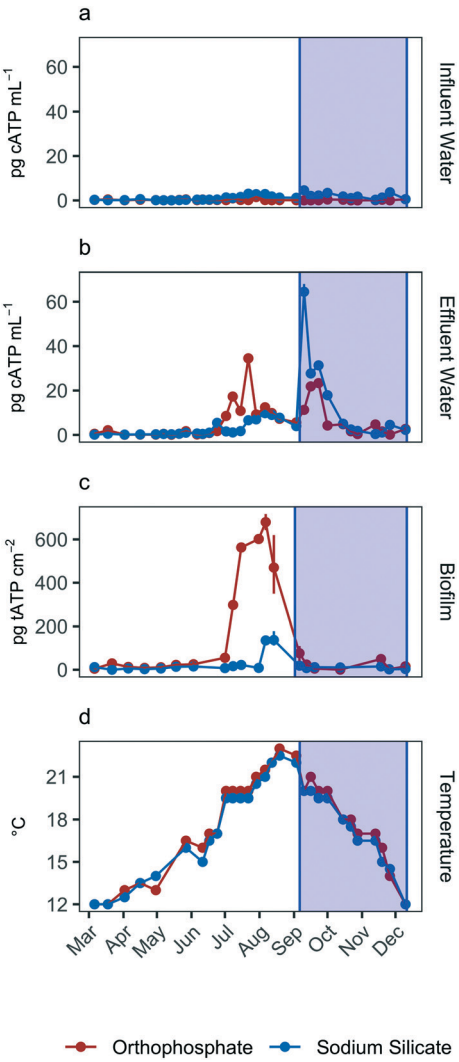

Fig. 2 Average influent and effluent ATP concentrations in pg cATP per mL (a and b), average biofilm ATP concentrations in pg tATP per cm^2 (c), and influent water temperature in degrees C (d). Error bars represent maximum and minimum values, with n = 2. The shaded area represents an increase in sodium silicate dose from 24 to 48 mg SiO_2 per L.

represents the maximum recorded cellular ATP concentration (68.0 pg cATP per mL); increasing the sodium silicate dose appeared to promote the dispersion and release of biofilm-bound cells from the coupons into the bulk water. This may be due to the dispersive effects of sodium silicate,[15] or the concomitant increase in pH, or both. But since a comparable increase in pH in the orthophosphate system at the end of November (Fig. S1†) was not accompanied by a spike in biofilm, it seems plausible that sodium silicate had a dispersive effect beyond its influence on pH.

Total ATP concentrations, which represent the total sessile biomass accumulated on the polycarbonate coupons, increased in both systems during the July–September quarter (Fig. 2c). The maximum biofilm ATP concentrations were recorded during the same quarter. Median concentrations

were 30.4 pg tATP per cm^2 (range: 0–717.0 pg tATP per cm^2, n = 46), and 10.6 pg tATP per cm^2 (range: 0–178.0 pg tATP per cm^2, n = 46) in biofilm samples recovered from the orthophosphate- and sodium silicate-treated reactors, respectively. Peak biofilm ATP concentrations from the silicate-treated AR were approximately 4 times lower than the corresponding peak representing the orthophosphate-treated AR. And while there was some overlap in the orthophosphate system's biofilm ATP and cellular ATP spikes, cellular ATP and biofilm ATP were not strongly correlated in general (orthophosphate = −0.23, sodium silicate = 0.07) (Fig. 2). The two microbial indicators appear to be governed by different mechanisms.

The increase in biomass concentrations in the orthophosphate-treated system is consistent with previous studies reporting an increase in microbial growth due to orthophosphate.[6–8,10,55,56] Lehtola *et al.*[7] reported an increase in biomass concentrations after adding as little as 1 μg P–PO_4^{3-} L to treated drinking water with no disinfectant residual and a background concentration of 0.19 μg P per L. And while Rompré *et al.*[2] and Kogo *et al.*[22] indicated that biofilm accumulation was not influenced by corrosion inhibitor type (sodium silicate or orthophosphate), the results from this study suggest the opposite: tATP concentrations were substantially lower in the silicate-treated AR compared to the orthophosphate-treated AR. A similar finding was documented by Aghasadeghi *et al.*,[18] who used a pilot-scale system with excavated lead service lines. In that study, heterotrophic plate counts were lower in pipe wall biofilm in the silicate-treated system compared with the orthophosphate-treated system.

The reasons for orthophosphate's effect are likely complex. Phosphorus is essential for the synthesis of ATP, DNA, RNA, and phospholipids,[57] and orthophosphate may increase disinfectant efficacy.[57] And while microbial growth in drinking water systems is often limited by the concentration of assimilable organic carbon, in some waters phosphorus appears to be the limiting nutrient.[6–8] The effect of orthophosphate may also depend on the substrate to which biofilm is attached: orthophosphate may cause a negative shift in the zeta potential of a particular substrate, making adhesion by negatively-charged bacteria less favourable.[58]

Influence of corrosion inhibitors on biofilm growth at lower water temperatures (reservoir-suspended coupons)

To monitor the biomass accumulated at low water temperatures (<20 °C), biofilm ATP was quantified on polycarbonate coupons submerged in the effluent reservoirs for each pipe loop. The average reservoir water temperature was 16.8 °C (range: 16.5–17.5 °C) and 17.3 (range: 17.0–18.0 °C) in the sodium silicate- and orthophosphate-treated systems, respectively.

Coupons removed from the sodium silicate-treated reservoirs had lower median ATP concentrations than those removed from the orthophosphate-treated reservoirs across both water main types (cast-iron and PVC) (Fig. 3). The median biofilm ATP concentrations representing the cast-iron pipe loop systems treated with sodium silicate and orthophosphate were 20.9 pg tATP per cm^2 (range: 9.62–55.2 pg tATP per cm^2, n = 12) and 31.8 pg tATP per cm^2 (range: 0.00–77.8 pg tATP per cm^2, n = 12), respectively. Similarly, the median biofilm ATP concentrations representing the PVC pipe loop systems treated with sodium silicate and orthophosphate were 18.2 pg tATP per cm^2 (range: 0.00–46.9 pg tATP per cm^2, n = 12) and 22.3 pg tATP per cm^2 (range: 9.14–79.5 pg tATP per cm^2, n = 12). However, a two-way ANOVA test with Tukey's HSD method conducted on the data set indicated that there were no significant differences in average biofilm ATP concentrations between the pipe materials or the corrosion inhibitor treatments (PVC–cast-iron CI: −14.9, 5.8 pg tATP per cm^2; sodium silicate– orthophosphate CI: −16.7, 3.9 pg tATP per cm^2).

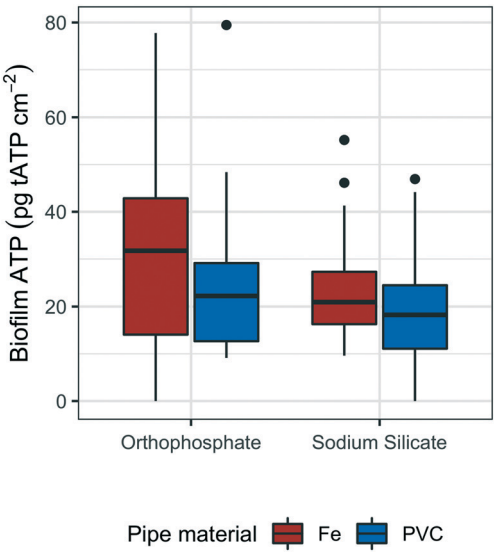

Fig. 3 Box plots of tATP measured on the coupons submerged in the reservoirs of each PVC and cast-iron pipe loop; n = 12 per group.

While not strongly evident in this study, pipe material does influence biofilm growth in drinking water systems.[59–63] For example, Niquette *et al.*[61] demonstrated that pipe material influenced the density of fixed biomass and that PVC, along with polyethylene, supported less fixed biomass than iron and cement-based materials. A similar, albeit weak, trend is shown in Fig. 3: median tATP concentrations representing cast-iron pipe loops were higher than those representing PVC.

Influence of corrosion inhibitors on biofilm growth at high-water temperatures (batch reactors)

The substantial difference between biofilm growth in the presence of sodium silicate and orthophosphate at water temperatures above 20 °C was confirmed using batch

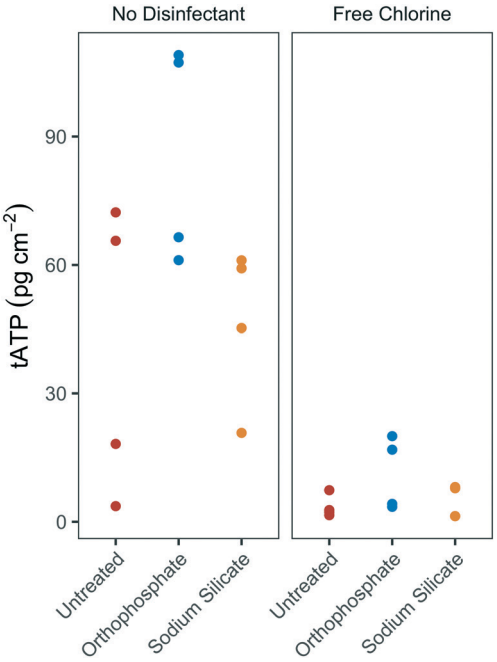

Fig. 4 tATP concentrations on annular PEX coupons in batch reactors with modified filtered water at 20 °C, with and without chlorine addition; n = 4 per group.

reactors with PEX coupons. While orthophosphate was associated with increased tATP concentrations on PEX pipe coupons, sodium silicate was not (Fig. 4). In the absence of disinfectant, the median biofilm ATP concentrations on the orthophosphate- and sodium silicate-treated coupons were 86.9 pg tATP per cm^2 (range: 61.1–109.0 pg tATP per cm^2, n = 4), and 52.2 pg tATP per cm^2 (20.8–61.1 pg tATP per cm^2), respectively.

Biofilm ATP surface concentrations were lower on coupons exposed to free chlorine, but the orthophosphate-treated coupons yielded higher median ATP values than the untreated and the sodium silicate-treated coupons (Fig. 4). These results complement the findings from the pilot-scale study in which higher biomass concentrations were measured in the orthophosphate-treated AR when water temperature increased above 20 °C during Q2 (July–September). A two-way ANOVA test with Tukey's HSD comparison confirmed that the average biofilm ATP concentrations were significantly different between the coupons that were treated with orthophosphate and the ones that did not have any corrosion control treatment (orthophosphate – untreated CI: 2.02–51.6 pg tATP per cm^2).

Temperature is known to have a positive effect on biofilm growth.[57] It affects the expression of genes linked to EPS formation and it impacts the hydrophobicity of cell surfaces.[57] In addition to its direct effects, higher temperatures increase chlorine demand, which may decrease the inhibition of biofilm growth by chlorine.[57] Thus, higher doses of disinfectant are usually necessary to control biofilm at elevated summer water temperatures.

Microbial community structure

Taxonomic analysis. Manganese-oxidizing bacteria (MOB) were more abundant in the sodium silicate-treated system compared to the orthophosphate-treated system. The genera *Hyphomicrobium* and *Sphingomonas*, which include manganese-oxidizing bacteria (MOB),[64,65] were present in both orthophosphate- and sodium silicate-treated systems (Fig. 5). The silicate-treated system had relative *Hyphomicrobium* abundances of 4.8% and 2.8% in June and July, respectively. In comparison, the highest abundance of *Hyphomicrobium* in the orthophosphate-treated system was 0.9% in December. *Hyphomicrobium* was previously identified in biofilms collected in ARs that were operated with untreated water from Pockwock Lake, the source water that was treated for this study (*i.e.*, raw water from JD Kline water supply plant).[66]

Similarly, the highest abundance of *Sphingomonas* was detected in samples from the silicate-treated AR collected in October (34.3%). In comparison, the highest relative abundance for this genus in the orthophosphate-treated AR occurred in September (15.8%). Known iron-oxidizing bacteria (FeOB) of the genera *Gallionella* and *Leptothrix*[67] were not identified in this study. Additional taxonomic profiles at the phylum level are summarized in Fig. S4.†

The genera *Mycobacterium* and *Halomonas*—which include pathogenic organisms—were more abundant in the presence of orthophosphate. *Legionella* and *Escherichia–Shigella* were identified at the genus level with low relative abundances (Tables S1 and S2†). The genus *Mycobacterium* is frequently detected in drinking water distribution systems and includes opportunistic pathogens and chlorine-resistant species.[68,69] The relative abundance of *Mycobacterium* was below 2% in the sodium silicate system, whereas the orthophosphate system yielded a relative *Mycobacterium* abundance above 3% in December. The genus *Halomonas*, which includes species of bacteria that may display pathogenic potential in humans,[70] was detected in the orthophosphate-treated system in each sampling month except June. In contrast, *Halomonas* were only detected in September, October, and November in the silicate-treated system. In November, the relative abundances of *Halomonas* increased to 7.5% and 1.9% in the orthophosphate- and sodium silicate-treated systems, respectively. The genus *Escherichia–Shigella*, which contains *Escherichia coli*, was detected, but with low frequency and lower abundance compared to *Halomonas* and *Mycobacterium*. The highest relative abundance for these genera occurred in November in the sodium silicate-treated AR at 0.6%. Furthermore, the genus *Legionella*, which includes the pathogenic species *Legionella pneumophila*, was also detected in both systems. However, while a low abundance was recorded (similar to *Mycobacterium* and *Halomonas*), the *Legionella* in the sodium silicate system was detected in September, October, and November with an increasing relative

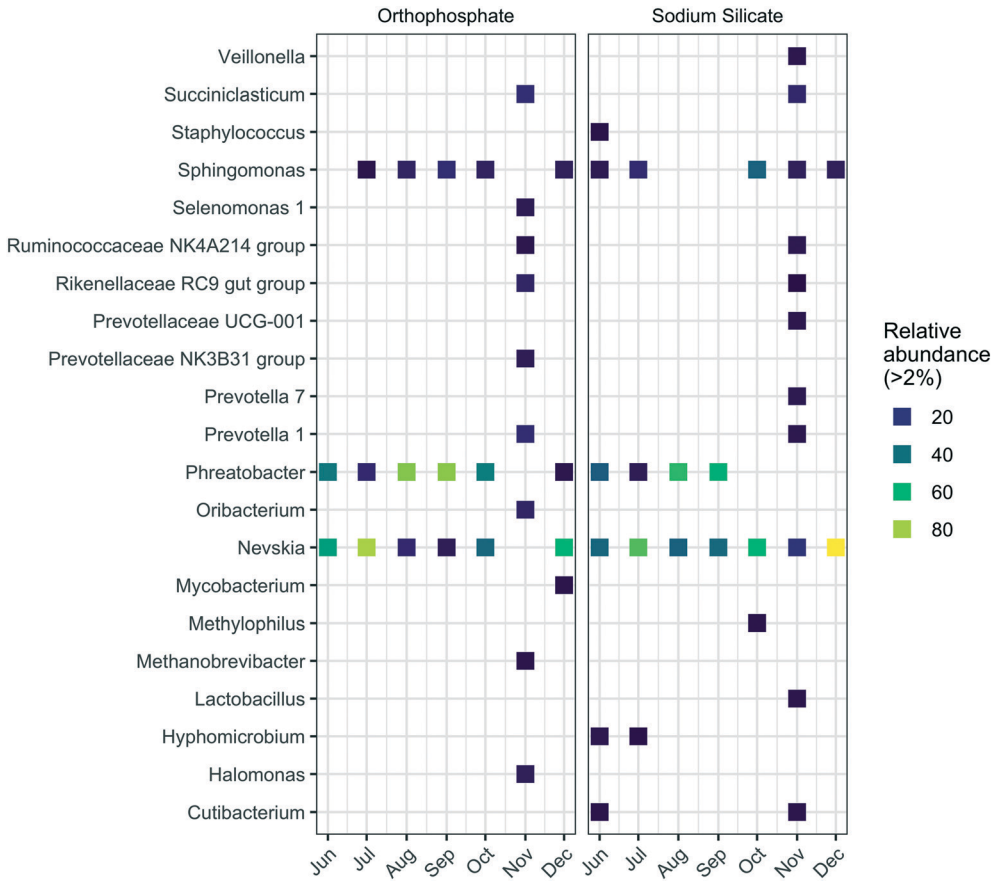

Fig. 5 Relative abundance of bacterial genera, by month.

abundance from month to month. Both *Mycobacterium* and *Legionella* have similar occurrence patterns in water distribution systems, interactions with protozoa, and tendency to form biofilms.[69,71,72]

Alpha and beta diversity analysis. In general, no significant differences in diversity and richness between the orthophosphate- and sodium silicate-treated groups were detected. The richness, Shannon diversity index, and Pielou's evenness index were calculated for every sequenced sample, and the alpha diversity indexes are summarized in Fig. S5.† The observed ASVs noticeably increased in November, which reflects the change in biofilm community composition in both systems. This shift was more evident in the orthophosphate-treated AR. Overall, biofilm samples demonstrated the highest evenness (Pielou's index) as well as the highest diversity (Shannon index) in November 2019. On average, the orthophosphate system exhibited higher microbial evenness (Pielou's index: 0.50) and diversity (Shannon index: 1.61) in comparison to the sodium silicate-treated system (Pielou's index: 0.44; Shannon index: 1.55). No significant differences in community structure between the orthophosphate- and the sodium silicate-treated groups were identified using the weighted (p = 0.75) or unweighted (p = 0.65) UniFrac methods (Fig. S6†).

Conclusion

The effects of sodium silicates on corrosion and biomass accumulation in drinking water distribution systems are poorly understood. The objective of this work was to compare sodium silicate and orthophosphate with respect to biofilm formation at constant pH. The results from this work suggest the following:

1. Orthophosphate promotes more biofilm growth than sodium silicate, but only at relatively high water temperatures. As shown in the results from the pilot study, the biofilm ATP concentrations on coupons recovered from the orthophosphate-treated AR were significantly higher than those from the sodium silicate-treated AR between July and September, when the water temperature exceeded 20 °C. Two separate experiments—involving (1) polycarbonate coupons exposed to treated water from the cast-iron and PVC pipe loops at lower water temperatures (below 20 °C) and (2) PEX coupons in batch reactors exposed to warmer water temperatures (20 °C)—corroborate the finding that biomass accumulated in the presence of orthophosphate at high water temperatures only. At low water temperatures (≲15 °C), there were no significant differences in average biofilm ATP concentrations regardless of the corrosion inhibitor treatment. However, the biofilm ATP concentrations recorded

in the batch reactors confirmed that, when the water temperature was maintained at 20 °C, more biomass accumulated on the orthophosphate-treated coupons.

2. A free chlorine residual had a substantial negative impact on biofilm ATP concentrations, and this was particularly noticeable in the presence of orthophosphate.

3. Effluent cATP concentrations spiked with the increase in sodium silicate dose from 24 to 48 mg SiO_2 per L. This suggests that changes in sodium silicate concentrations disturbed and dispersed the biofilm formed inside the AR. This may present a risk when sodium silicate is used as a water treatment additive.

4. Orthophosphate promoted biofilm growth, but it did not disrupt the community structure in comparison to the biofilms exposed to sodium silicate. Genera that include opportunistic pathogens—*Mycobacterium*, *Halomonas*, *Escherichia*, and *Legionella*—were detected in both systems. The genera *Halomonas* and *Mycobacterium* were present at greater relative abundances in the orthophosphate-treated system in comparison to the sodium silicate system. Conversely, *Escherichia* and *Legionella* were more abundant on sodium silicate-treated coupons. Even though these genera were detected, it was not possible to identify organisms at the species level.

Author contributions

Sebastian Munoz and Bofu Li carried out the experiments. Sebastian Munoz processed the experimental data, performed the analysis, and designed the figures. Sebastian Munoz and Benjamin F. Trueman wrote the manuscript with support from Bofu Li and Graham A. Gagnon. Benjamin F. Trueman supported the data analysis. Graham A. Gagnon supervised the project.

Conflicts of interest

This work was partially funded by National Silicates.

Acknowledgements

This work was funded by an NSERC CRD grant (CRDPJ 509252-17) in collaboration with National Silicates and Cold-Block Technologies; additional funding support was provided through the NSERC/Halifax Water Industrial Research Chair program (IRCPJ 349838-16) and the Mitacs Accelerate program (Reference # IT23352). We acknowledge the technical expertise provided by Heather Daurie (Centre for Water Resources Studies), Andrew Houlihan (Halifax Water), Jessica Campbell (Halifax Water), Nicole Allward (Centre for Water Resources Studies), Amy Murdock, and James Dalton.

References

1 M. W. LeChevallier, N. J. Welch and D. B. Smith, Full-scale studies of factors related to coliform regrowth in drinking water, *Appl. Environ. Microbiol.*, 1996, **62**, 2201–2211.

2 A. Rompré, M. Prévost, J. Coallier, P. Brisebois and J. Lavoie, Impacts of implementing a corrosion control strategy on biofilm growth, *Water Sci. Technol.*, 2000, **41**, 287–294.

3 I. Douterelo, S. Husband and J. B. Boxall, The bacteriological composition of biomass recovered by flushing an operational drinking water distribution system, *Water Res.*, 2014, **54**, 100–114.

4 T. S. Munasinghe, C. L. Abayasekara, A. Jayawardana and R. Chandrajith, The effect of iron corrosion in cast iron pipes on the microbiological quality of drinking water: a laboratory and field investigation, *Ceylon Journal of Science*, 2017, **46**, 99.

5 R. B. Arnold, B. Rosenfeldt, J. Rhoades, C. Owen and W. Becker, Evolving utility practices and experiences with corrosion control, *J. - Am. Water Works Assoc.*, 2020, **112**(7), 26–40.

6 W. Fang, J. Y. Hu and S. L. Ong, Influence of phosphorus on biofilm formation in model drinking water distribution systems, *J. Appl. Microbiol.*, 2009, **106**, 1328–1335.

7 M. J. Lehtola, I. T. Miettinen and P. J. Martikainen, Biofilm formation in drinking water affected by low concentrations of phosphorus, *Can. J. Microbiol.*, 2002, **48**, 494–499.

8 I. T. Miettinen, T. Vartiainen and P. J. Martikainen, Phosphorus and bacterial growth in drinking water, *Appl. Environ. Microbiol.*, 1997, **63**, 3242–3245.

9 A. Sathasivan and S. Ohgaki, Application of new bacterial regrowth potential method for water distribution system - A clear evidence of phosphorus limitation, *Water Res.*, 1999, **33**, 137–144.

10 H. J. Jang, Y. J. Choi, H. M. Ro and J. O. Ka, Effects of phosphate addition on biofilm bacterial communities and water quality in annular reactors equipped with stainless steel and ductile cast iron pipes, *J. Microbiol.*, 2012, **50**, 17–28.

11 X. Li, G. Upadhyaya, W. Yuen, J. Brown, E. Morgenroth and L. Raskin, Changes in the structure and function of microbial communities in drinking water treatment bioreactors upon addition of phosphorus, *Appl. Environ. Microbiol.*, 2010, **76**, 7473–7481.

12 M. Gouider, J. Bouzid, S. Sayadi and A. Montiel, Impact of orthophosphate addition on biofilm development in drinking water distribution systems, *J. Hazard. Mater.*, 2009, **167**, 1198–1202.

13 M. Batté, L. Mathieu, P. Laurent and M. Prévost, Influence of phosphate and disinfection on the composition of biofilms produced from drinking water, as measured by fluorescence in situ hybridization, *Can. J. Microbiol.*, 2003, **49**, 741–753.

14 D. A. Lytle, M. R. Schock, C. Formal, C. Bennett-Stamper, S. Harmon, M. N. Nadagouda, D. Williams, M. K. DeSantis, J. Tully and M. Pham, Lead Particle Size Fractionation and Identification in Newark, New Jersey's Drinking Water, *Environ. Sci. Technol.*, 2020, **54**, 13672–13679.

15 B. Li, B. F. Trueman, S. Munoz, J. M. Locsin and G. A. Gagnon, Impact of sodium silicate on lead release and colloid size distributions in drinking water, *Water Res.*, 2021, **190**, 116709.

16 R. B. Robinson, G. D. Reed and B. Frazier, Iron and manganese sequestration facilities using sodium silicate, *J. - Am. Water Works Assoc.*, 1992, **84**, 77–82.
17 M. Woszczynski, J. Bergese, S. J. Payne and G. A. Gagnon, Comparison of sodium silicate and phosphate for controlling lead release from copper pipe rigs, *Can. J. Civ. Eng.*, 2015, **42**, 953–959.
18 K. Aghasadeghi, S. Peldszus, B. F. Trueman, A. Mishrra, M. G. Cooke, R. M. Slawson, D. E. Giammar, G. A. Gagnon and P. M. Huck, Pilot-scale comparison of sodium silicates, orthophosphate and pH adjustment to reduce lead release from lead service lines, *Water Res.*, 2021, **195**, 116955.
19 A. Mishrra, Z. Wang, V. Sidorkiewicz and D. E. Giammar, Effect of sodium silicate on lead release from lead service lines, *Water Res.*, 2021, **188**, 116485.
20 A. S. Kinsela, A. M. Jones, M. W. Bligh, A. N. Pham, R. N. Collins, J. J. Harrison, K. L. Wilsher, T. E. Payne and T. D. Waite, Influence of Dissolved Silicate on Rates of Fe(II) Oxidation, *Environ. Sci. Technol.*, 2016, **50**, 11663–11671.
21 B. Li, B. F. Trueman, M. S. Rahman, Y. Gao, Y. Park and G. A. Gagnon, Understanding the impacts of sodium silicate on water quality and iron oxide particles, *Environ. Sci.: Water Res. Technol.*, 2019, **5**, 1360–1370.
22 A. Kogo, S. J. Payne and R. C. Andrews, Comparison of three corrosion inhibitors in simulated partial lead service line replacements, *J. Hazard. Mater.*, 2017, 211–221.
23 A. D. Knowles, J. Mackay and G. A. Gagnon, Pairing a pilot plant to a direct filtration water treatment plant, *Can. J. Civ. Eng.*, 2012, **39**, 689–700.
24 A. K. Stoddart and G. A. Gagnon, Full-scale prechlorine removal: Impact on filter performance and water quality, *J. - Am. Water Works Assoc.*, 2015, **107**, E638–E647.
25 G. A. Gagnon and J. D. Doubrough, Lead release from premise plumbing: A profile of sample collection and pilot studies from a small system, *Can. J. Civ. Eng.*, 2011, **38**, 741–750.
26 M. Woszczynski, J. Bergese and G. A. Gagnon, Comparison of chlorine and chloramines on lead release from copper pipe rigs, *J. Environ. Eng.*, 2013, **139**, 1099–1107.
27 B. F. Trueman and G. A. Gagnon, Understanding the Role of Particulate Iron in Lead Release to Drinking Water, *Environ. Sci. Technol.*, 2016, **50**, 9053–9060.
28 J. Tully, M. K. DeSantis and M. R. Schock, Water quality–pipe deposit relationships in Midwestern lead pipes, *AWWA Water Sci.*, 2019, **1**, e1127.
29 B. Li, B. F. Trueman, E. Doré and G. A. Gagnon, Effectiveness of Sodium Silicates for Lead Corrosion Control: A Critical Review of Current Data, *Environ. Sci. Technol. Lett.*, 2021, **8**, 932–939.
30 G. A. Gagnon and R. M. Slawson, An efficient biofilm removal method for bacterial cells exposed to drinking water, *J. Microbiol. Methods*, 1999, **34**, 203–214.
31 H. M. Murphy, S. J. Payne and G. A. Gagnon, Sequential UV- and chlorine-based disinfection to mitigate Escherichia coli in drinking water biofilms, *Water Res.*, 2008, **42**, 2083–2092.
32 J. L. Rand, R. Hofmann, M. Z. B. Alam, C. Chauret, R. Cantwell, R. C. Andrews and G. A. Gagnon, A field study evaluation for mitigating biofouling with chlorine dioxide or chlorine integrated with UV disinfection, *Water Res.*, 2007, **41**, 1939–1948.
33 Y. Zhu, H. Wang, X. Li, C. Hu, M. Yang and J. Qu, Characterization of biofilm and corrosion of cast iron pipes in drinking water distribution system with UV/Cl2 disinfection, *Water Res.*, 2014, **60**, 174–181.
34 S. K. Park, Y. K. Kim, Y. S. Oh and S. C. Choi, Growth kinetics and chlorine resistance of heterotrophic bacteria isolated from young biofilms formed on a model drinking water distribution system, *Korean J. Microbiol.*, 2015, **51**, 355–363.
35 A. C. Pavarina, L. N. Dovigo, P. V. Sanita, A. L. Machado, E. T. Giampaolo and C. E. Vergani, in *Biofilms: Formation, development and properties*, 1st edn, 2011.
36 S. L. Gora, K. D. Rauch, C. C. Ontiveros, A. K. Stoddart and G. A. Gagnon, Inactivation of biofilm-bound Pseudomonas aeruginosa bacteria using UVC light emitting diodes (UVC LEDs), *Water Res.*, 2019, **151**, 193–202.
37 A. M. Comeau, G. M. Douglas and M. G. I. Langille, Microbiome Helper: a Custom and Streamlined Workflow for Microbiome Research, *mSystems*, 2017, **2**, 1–11.
38 M. Martin, The relationship between organizational culture and knowledge management, & their simultaneous effects on customer relation management, *EMBnet.journal*, 2011, **17**, 10–12.
39 E. Bolyen, J. R. Rideout, M. R. Dillon, N. A. Bokulich, C. C. Abnet, G. A. Al-Ghalith, H. Alexander, E. J. Alm, M. Arumugam, F. Asnicar, Y. Bai, J. E. Bisanz, K. Bittinger, A. Brejnrod, C. J. Brislawn, C. T. Brown, B. J. Callahan, A. M. Caraballo-Rodríguez, J. Chase, E. K. Cope, R. Da Silva, C. Diener, P. C. Dorrestein, G. M. Douglas, D. M. Durall, C. Duvallet, C. F. Edwardson, M. Ernst, M. Estaki, J. Fouquier, J. M. Gauglitz, S. M. Gibbons, D. L. Gibson, A. Gonzalez, K. Gorlick, J. Guo, B. Hillmann, S. Holmes, H. Holste, C. Huttenhower, G. A. Huttley, S. Janssen, A. K. Jarmusch, L. Jiang, B. D. Kaehler, K. B. Kang, C. R. Keefe, P. Keim, S. T. Kelley, D. Knights, I. Koester, T. Kosciolek, J. Kreps, M. G. I. Langille, J. Lee, R. Ley, Y.-X. Liu, E. Loftfield, C. Lozupone, M. Maher, C. Marotz, B. D. Martin, D. McDonald, L. J. McIver, A. V. Melnik, J. L. Metcalf, S. C. Morgan, J. T. Morton, A. T. Naimey, J. A. Navas-Molina, L. F. Nothias, S. B. Orchanian, T. Pearson, S. L. Peoples, D. Petras, M. L. Preuss, E. Pruesse, L. B. Rasmussen, A. Rivers, M. S. Robeson, P. Rosenthal, N. Segata, M. Shaffer, A. Shiffer, R. Sinha, S. J. Song, J. R. Spear, A. D. Swafford, L. R. Thompson, P. J. Torres, P. Trinh, A. Tripathi, P. J. Turnbaugh, S. Ul-Hasan, J. J. J. van der Hooft, F. Vargas, Y. Vázquez-Baeza, E. Vogtmann, M. von Hippel, W. Walters, Y. Wan, M. Wang, J. Warren, K. C. Weber, C. H. D. Williamson, A. D. Willis, Z. Z. Xu, J. R. Zaneveld, Y. Zhang, Q. Zhu, R. Knight and J. G. Caporaso, Reproducible, interactive, scalable and extensible microbiome data science using QIIME 2, *Nat. Biotechnol.*, 2019, **37**, 852–857.

40 B. J. Callahan, P. J. McMurdie, M. J. Rosen, A. W. Han, A. J. A. Johnson and S. P. Holmes, DADA2: High-resolution sample inference from Illumina amplicon data, *Nat. Methods*, 2016, **13**, 581–583.

41 A. Amir, M. Daniel, J. Navas-Molina, E. Kopylova, J. Morton, Z. Z. Xu, K. Eric, L. Thompson, E. Hyde, A. Gonzalez and R. Knight, Deblur Rapidly Resolves Single, *mSystems*, 2017, **2**, 1–7.

42 K. Katoh and H. Toh, Parallelization of the MAFFT multiple sequence alignment program, *Bioinformatics*, 2010, **26**, 1899–1900.

43 C. Quast, E. Pruesse, P. Yilmaz, J. Gerken, T. Schweer, P. Yarza, J. Peplies and F. O. Glöckner, The SILVA ribosomal RNA gene database project: Improved data processing and web-based tools, *Nucleic Acids Res.*, 2013, **41**, 590–596.

44 P. J. McMurdie and S. Holmes, Phyloseq: An R Package for Reproducible Interactive Analysis and Graphics of Microbiome Census Data, *PLoS One*, 2013, **8**(4), e61217.

45 *4500-Cl Chlorine (residual)*, Standard methods for the examination of water and wastewater, **https://www.standardmethods.org/doi/abs/10.2105/SMWW.2882.078**.

46 *4500-P Phosphorus*, Standard methods for the examination of water and wastewater, **https://www.standardmethods.org/doi/abs/10.2105/SMWW.2882.093**.

47 *Hach*, Silicomolybdate method, Method 8185, DOC316.53.01133, **www.hach.com/asset-get.download.jsa?id=7639983849**.

48 H. Wickham, M. Averick, J. Bryan, W. Chang, L. D. McGowan, R. François, G. Grolemund, A. Hayes, L. Henry, J. Hester, M. Kuhn, T. L. Pedersen, E. Miller, S. M. Bache, K. Müller, J. Ooms, D. Robinson, D. P. Seidel, V. Spinu, K. Takahashi, D. Vaughan, C. Wilke, K. Woo and H. Yutani, Welcome to the tidyverse, *J. Open Source Softw.*, 2019, **4**, 1686.

49 S. Garnier, N. Ross, R. Rudis, A. P. Camargo, M. Sciaini and C. Scherer, *viridis - colorblind-friendly color maps for r*, **https://sjmgarnier.github.io/viridis/**.

50 J. Oksanen, F. G. Blanchet, M. Friendly, R. Kindt, P. Legendre, D. McGlinn, P. R. Minchin, R. B. O'Hara, G. L. Simpson, P. Solymos, M. H. H. Stevens, E. Szoecs and H. Wagner, *Vegan*, **https://CRAN.R-project.org/package=vegan**.

51 P. O'Shaughnessy and J. E. Cavanaugh, Performing t-tests to compare autocorrelated time series data collected from direct-reading instruments, *J. Occup. Environ. Hyg.*, 2015, **12**, 743–752.

52 Q. Chang, Y. Luan and F. Sun, Variance adjusted weighted UniFrac: A powerful beta diversity measure for comparing communities based on phylogeny, *BMC Bioinf.*, 2011, **12**, 118.

53 C. Lozupone, M. E. Lladser, D. Knights, J. Stombaugh and R. Knight, UniFrac: An effective distance metric for microbial community comparison, *ISME J.*, 2011, **5**, 169–172.

54 M. J. Anderson, Permutational Multivariate Analysis of Variance (PERMANOVA), *Wiley StatsRef, Statistics Reference Online*, 2017, pp. 1–15.

55 C. Chu, C. Lu and C. Lee, Effects of inorganic nutrients on the regrowth of heterotrophic bacteria in drinking water distribution systems, *J. Environ. Manage.*, 2005, **74**, 255–263.

56 S. J. Payne, G. S. Piorkowski, L. T. Hansen and G. A. Gagnon, Impact of zinc orthophosphate on simulated drinking water biofilms influenced by lead and copper, *J. Environ. Eng.*, 2016, **142**, 1–9.

57 S. Liu, C. Gunawan, N. Barraud, S. A. Rice, E. J. Harry and R. Amal, Understanding, Monitoring, and Controlling Biofilm Growth in Drinking Water Distribution Systems, *Environ. Sci. Technol.*, 2016, **50**, 8954–8976.

58 B. M. R. Appenzeller, Y. B. Duval, F. Thomas and J.-C. Block, Influence of Phosphate on Bacterial Adhesion onto Iron Oxyhydroxide in Drinking Water, *Environ. Sci. Technol.*, 2002, **36**, 646–652.

59 Y. C. Chang, M. Le Puil, J. Biggerstaff, A. A. Randall, A. Schulte and J. S. Taylor, Direct estimation of biofilm density on different pipe material coupons using a specific DNA-probe, *Mol. Cell. Probes*, 2003, **17**, 237–243.

60 R. Liu, J. Zhu, Z. Yu, D. R. Joshi, H. Zhang, W. Lin and M. Yang, Molecular analysis of long-term biofilm formation on PVC and cast iron surfaces in drinking water distribution system, *J. Environ. Sci.*, 2014, **26**, 865–874.

61 P. Niquette, P. Servais and R. Savoir, Impacts of pipe materials on densities of fixed bacterial biomass in a drinking water distribution system, *Water Res.*, 2000, **34**, 1952–1956.

62 C. D. Norton and M. W. LeChevallier, A pilot study of bacteriological population changes through potable water treatment and distribution, *Appl. Environ. Microbiol.*, 2000, **66**, 268–276.

63 T. Schwartz, S. Hoffmann and U. Obst, Formation and bacterial composition of young, natural biofilms obtained from public bank-filtered drinking water systems, *Water Res.*, 1998, **32**, 2787–2797.

64 P. Mouchet, From conventional to biological removal of iron and manganese in France, *J. - Am. Water Works Assoc.*, 1992, **84**, 158–167.

65 P. Yli-Hemminki, K. S. Jørgensen and J. Lehtoranta, Iron-Manganese Concretions Sustaining Microbial Life in the Baltic Sea: The Structure of the Bacterial Community and Enrichments in Metal-Oxidizing Conditions, *Geomicrobiol. J.*, 2014, **31**, 263–275.

66 N. E. Allward, B. S. Gregory, A. K. Sotddart and G. A. Gagnon, Potential for manganese biofouling in water transmission lines using model reactors, *Environ. Sci.: Water Res. Technol.*, 2018, **4**, 761–772.

67 S. Hedrich, M. Schlömann and D. Barrie Johnson, The iron-oxidizing proteobacteria, *Microbiology*, 2011, **157**, 1551–1564.

68 I. Douterelo, S. Husband, V. Loza and J. Boxall, Dynamics of biofilm regrowth in drinking water distribution systems, *Appl. Environ. Microbiol.*, 2016, **82**, 4155–4168.

69 M. J. M. Vaerewijck, G. Huys, J. C. Palomino, J. Swings and F. Portaels, Mycobacteria in drinking water distribution systems: Ecology and significance for human health, *FEMS Microbiol. Rev.*, 2005, **29**, 911–934.

70 D. A. Stevens, J. R. Hamilton, N. Johnson, K. K. Kim and J. S. Lee, Halomonas, a newly recognized human pathogen causing infections and contamination in a dialysis center: Three new species, *Medicine*, 2009, **88**, 244–249.

71 M. Pryor, S. Springthorpe, S. Riffard, T. Brooks, Y. Huo, G. Davis and S. A. Sattar, Investigation of opportunistic pathogens in municipal drinking water under different supply and treatment regimes, *Water Sci. Technol.*, 2004, **50**, 83–90.

72 T. Schwartz, S. Hoffmann and U. Obst, Formation of natural biofilms during chlorine dioxide and u.v. disinfection in a public drinking water distribution system, *J. Appl. Microbiol.*, 2003, **95**, 591–601.